Proceedings of the 1st Joint Symposium on the Natural History and Geology of The Bahamas

June 12-16, 2015

Gerace Research Centre
University of The Bahamas
San Salvador, The Bahamas

Conference Organizer:
Thomas A. Rothfus

Content Editors:
Carol L. Landry
Dan S. Kjar

Production Editors:
Lee J. Florea
Carol L. Landry

Gerace Research Centre
San Salvador, Bahamas
2017

ISBN: 978-0-935909-40-1

Cover image - Patch reef near the wall off Grotto Beach (photo by Lee Florea).

Preliminary geophysical imaging of nearshore tidal pumping on San Salvador Island utilizing time lapse electrical resistivity tomography

Lee J. Florea[1], Dan L. Rust[2], and Devyn J. Unger[2]

[1]Indiana Geological Survey, Indiana University, Bloomington, IN
[2]Department of Geological Sciences, Ball State University, Muncie, IN

1. Abstract

Electrical resistivity tomography profiles were collected on January 4, 2014 near the Government Dock in Graham's Harbour on San Salvador Island, Bahamas. These data include 11 sets of replicate profiles taken at approximately 30-minute intervals using a 28 electrode AGI Supersting R1/IP (with a 2 meter spacing in a Schlumberger array configuration). The goal of the study was to gauge the magnitude of tidal pumping on the nearshore groundwater environment of this carbonate island. Measurements spanned one half of a tidal cycle from an hour before high tide until low tide.

Comparing resistance data for each dataset against the initial dataset, we demonstrate that bulk resistance decreased sequentially to a minimum of 11.5% below the initial configuration during the measurement period. The timing of the changes suggests that tidal pumping of seawater into the nearshore groundwater reaches a maximum 3 hours after high tide. Inversion models illustrate the spatial arrangement of changes to earth resistivity during the tidal cycle. Difference plots between each modeled dataset and the initial modeled data reveal that changes to resistivity are restricted to the upper 5 meters, are expectedly more pronounced closer to the shoreline, and are spatially arranged to demonstrate the rapid propagation of a pressure wave and delayed solute transport by advection and dispersion.

2. Introduction

Concerns regarding global climate change are broad reaching and include the plight of carbonate islands, such as San Salvador, which generally span a limited elevation range and thus dramatically reduce in size with small increases in eustatic sea level (Vacher and Quinn 2004, and references therein). The spatial extent and thickness of the freshwater lens underlying carbonate islands (Vacher 1988) can also significantly decrease with small rises in sea level, particularly in regions of negative water budgets (Sealey 1994; Mylroie et al. 1995; Crump and Gamble 2006), resulting in increased pressure on limited water resources (Erdman et al. 1997; Roebuck et al. 2004). Thus, it is highly relevant as part of our global climate outlook to better understand the dynamic response of the freshwater lens to fluctuations in sea level driven by periodic forcing, such as tides and seasonal cycles of precipitation, and intermittent storm surges.

The nearshore environment of carbonate islands, in addition to serving as the seepage face for submarine groundwater discharge, undergoes daily variation from tides and the dampened penetration of the tidal pulse into the nearshore aquifer matrix is a well understood phenomena that has been mathematically modeled in a homogeneous isotropic media (Townley 1995) and measured extensively at the diurnal (Li et al. 2009) and seasonal timescale (Michael et al. 2005). This tidal pulse can cause periodic rise and fall of the water table and capillary fringe and be an important driver of geochemical mixing between marine and meteoric waters. The combined effects of mixing and variable saturation states in nearshore deposits have a strong influence on eogenetic diagenesis, including cementation

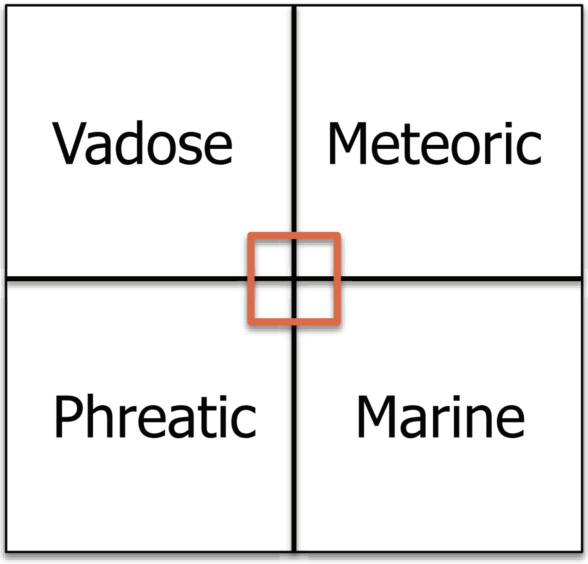

Figure 1. Diagenetic zones in eogenetic carbonates. Intersections between these zones (e.g., between meteoric and marine or between vadose and phreatic) are the locus of enhanced geochemical activity. The margin of the freshwater lens at the shoreline is at the intersection of all four diagenetic zones and is represented by the central square.

and the conversion of primary porosity to secondary permeability (Vacher et al. 1992; Whitaker and Smart 2004; Figure 1).

Electrical resistivity tomography (ERT) is one method that may be used to image the freshwater lens in coastal landscapes (Kruse et al. 1998; Urish and Frohlich 2009), whereby the potential difference and current generated by permutations of a series of electrodes develop a 'picture' of the subsurface composition through an inversion model of apparent resistivity data. Interpretation of the composition is guided by understanding the field setting and by applying Archie's Law (Archie 1952), which states that the modeled resistivity will be proportional to the fluid resistivity and inversely related to the saturation state and porosity. In other words, a coastal setting of generally homogeneous carbonate sand (such as an accretionary strand plain) will have three primary modes of resistivity: dry to moist sand (vadose zone – 10^3-10^4 $\Omega \cdot$m); the freshwater lens (meteoric phreatic zone – 10^1-10^3 $\Omega \cdot$m); and the underlying marine waters below the freshwater lens (marine phreatic zone – $10^{0.1}$-10^1 $\Omega \cdot$m).

Geo-electric methods have been used in North Andros Island, Bahamas to delineate the extent of freshwater resources (Wolfe et al. 2001) and identify the presence of karst features (Culpepper 2001). Previously on San Salvador, geo-electric methods have been used in the Cockburn Town well field (Kunze et al. 1994; Kunze et al. 1991; Gross and Kunze 1991), near Sandy Point (Kunze et al. 1989), and near Sandy Hook (Kunze and Weir 1986). These early studies utilized a simple four-electrode Schlumberger configuration to conduct depth profiles of resistivity and thus demarcate the top of the water table and the base of the freshwater lens at specific locations in Late Pleistocene (Cockburn Town) and Holocene (Sandy Point and Sandy Hook) strata.

More recently, ERT was utilized at the Line Hole well field by Russell et al. (2010). In this study, an early model Advanced Geosciences Inc. (AGI) R1 Earth Resistivity Meter with 28 electrodes was utilized in a dipole-dipole configuration to produce a modeled resistivity transect. Dipole-dipole electrode configurations differ from Schlumberger arrays in the arrangement and spacing of the current and potential difference electrode; whereas Schlumberger arrays are better at resolving depth profiles of resistivity, dipole-dipole arrays better resolve lateral variations in earth resistivity. RMS errors in the modeled profiles were higher than desired in the Line Hole study (>20%) due to difficulties with the equipment and the software resolving the strong contrast of apparent resistivity in the transect. However, this study did clearly identify a freshwater lens in the Holocene strand plain shoreward of the well field. The modeled freshwater lens appeared to thicken at the inland margin of the profile.

This study reports on recent attempts to image the freshwater lens using ERT on San Salvador Island near the Gerace Research Centre on Holocene sediments of an accretionary strand plain. In particular, we employ a time-lapse methodology (Meyerhoff

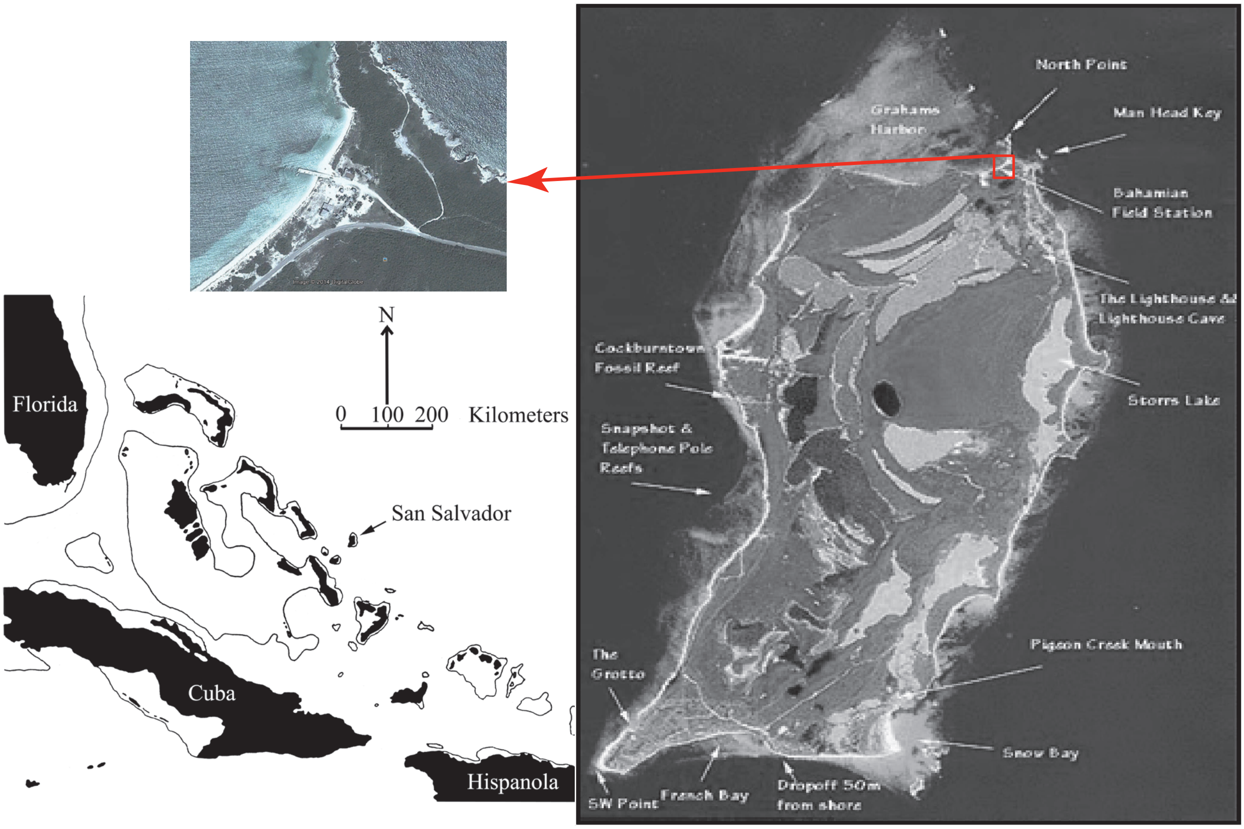

Figure 2. The Bahamas Archipelago, the island of San Salvador, and the location of the geophysical investigation at the Government Dock in Graham's Harbour. Inset image data: Google and DigitalGlobe.

et al. 2015; Yulia 2011; Tucker 2013) to assess changes in modeled profiles of earth resistivity during the course of a tidal cycle. The time-lapse method, in addition to identifying the bulk change in apparent resistivity between time steps, can pinpoint the coordinates in the ERT transect where such changes occur. These data can be one method to measure the attenuation of the tidal pulse, identify the spatial range of geochemical mixing, and compute the lag time between the tidal pulse and changes in the nearshore aquifer matrix.

3. Methods

ERT profiles were collected on January 4, 2014 near the Government Dock in Graham's Harbour on San Salvador Island, Bahamas (24.123°N, 74.458°W; Figure 2). These data include 11 sets of replicate profiles taken at approximately 30-minute intervals using an AGI SuperSting R1/IP with 28 passive electrodes. The gap between runs 4 and 5 aligns with the lunch period at the Gerace Research Centre. The electrodes were oriented perpendicular to the shoreline on a 2-m spacing with electrode 28 located just below the high-tide mark. The command sequence of the electrodes was organized in a Schlumberger array configuration to maximize the vertical resolution of changes to resistivity. Measurements spanned one half of a tidal cycle from an hour before high tide until low tide.

The data files from each profile (in AGI format) were converted in MatLab to a text format delimited in such a way to be read by the finite-element inversion modeling software R2 (version 2.7a; Binley and Kemma 2005). From these text files, the sum of the resistance data for each electrode configuration was computed. In R2, the profile for modeled resistivity was generated through iterative inverse modeling of the apparent resistivity data (the model grid had a horizontal resolution of 0.25 m and a vertical resolution of 0.5 m with a scaling factor of 1.1).

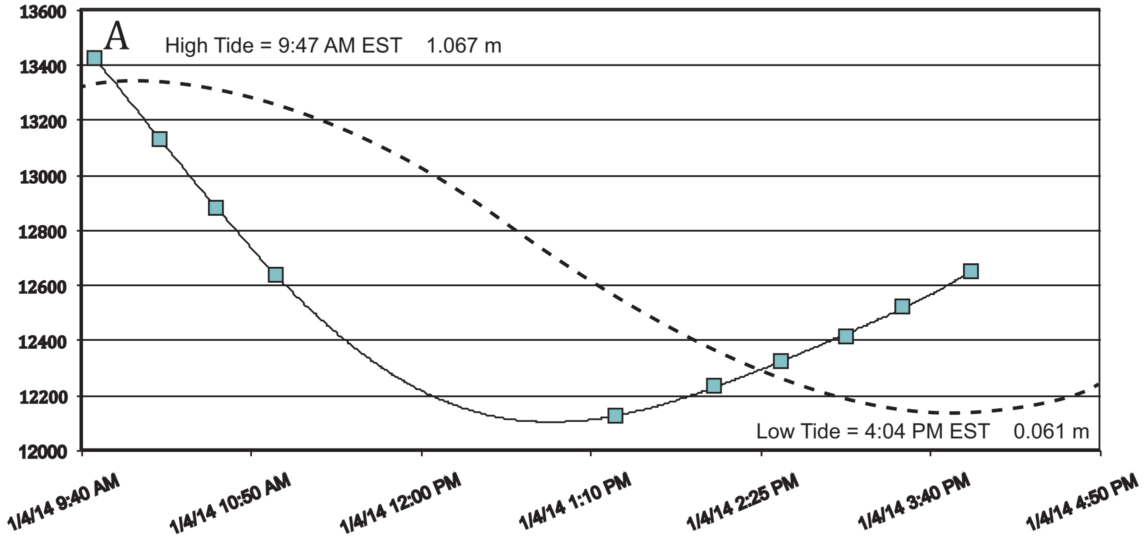

Figure 3. Time series of the sum of raw resistance values in the array file from each time step. Vertical axis is in Ohms and horizontal axis is in time. Dashed line is an overlay of the published tide chart for San Salvador with high and low tide times and range labeled (source: http://tides.mobilegeographics.com/locations/5570.html).

Also in R2, a difference inversion of modeled resistivity was created between the initial condition and each subsequent time step.

4. Results and Discussion

A time series of bulk resistance data are presented in Figure 3. Comparing each time step against the data from the initial dataset, the bulk resistance seemingly decreased sequentially to a minimum of 11.5% below the initial configuration at approximately three hours after high tide. The timing of the changes suggests one of two possibilities: 1) tidal forcing of seawater into nearshore groundwater, or 2) tidal oscillation of the water table; in both cases delayed by the attenuation of the aquifer matrix.

Inversion models of sequential profiles (Figure 4) all have RMS errors less than 5% and illustrate the spatial arrangement of earth resistivity during the time series of measurements. The highest values of modeled resistivity ($>10^3\ \Omega\cdot m$) are restricted to the upper 1.5 m of the profiles and inland of the electrodes in the swash zone; they are likely representative of the vadose zone of the strand plain. Middle range values of modeled resistivity (10^1-$10^3\ \Omega\cdot m$) occur as a shoreward thickening wedge at depths between 1.5 and 5 m below the surface and are most likely the freshwater lens, the capillary fringe, and overlying sand that experiences variable saturation due to tidal oscillation and meteoric recharge. The lowest values of modeled resistivity ($<10^1\ \Omega\cdot m$) occur below depth of 5 m and along the shore face and represent the marine phreatic zone of the coastal aquifer.

Difference plots between the modeled resistivity of each dataset and the initial data reveal significant changes to resistivity (Figure 5). The most significant increases in modeled resistivity (>30%) occur within the top meter of the profile and along the shore face, and are more pronounced in later time steps. These increases are most likely a lowering of the water table in response to, and in phase with, lower sea levels during low tide. In essence, they represent the rapid transmission of, and response to, a pressure wave through the nearshore aquifer.

Significant decreases in modeled resistivity (>5%) are restricted to the upper 5 m of the aquifer, are widespread, and therefore overwhelm the more restricted increases of resistivity within the model space (Figure 5). They are also out of

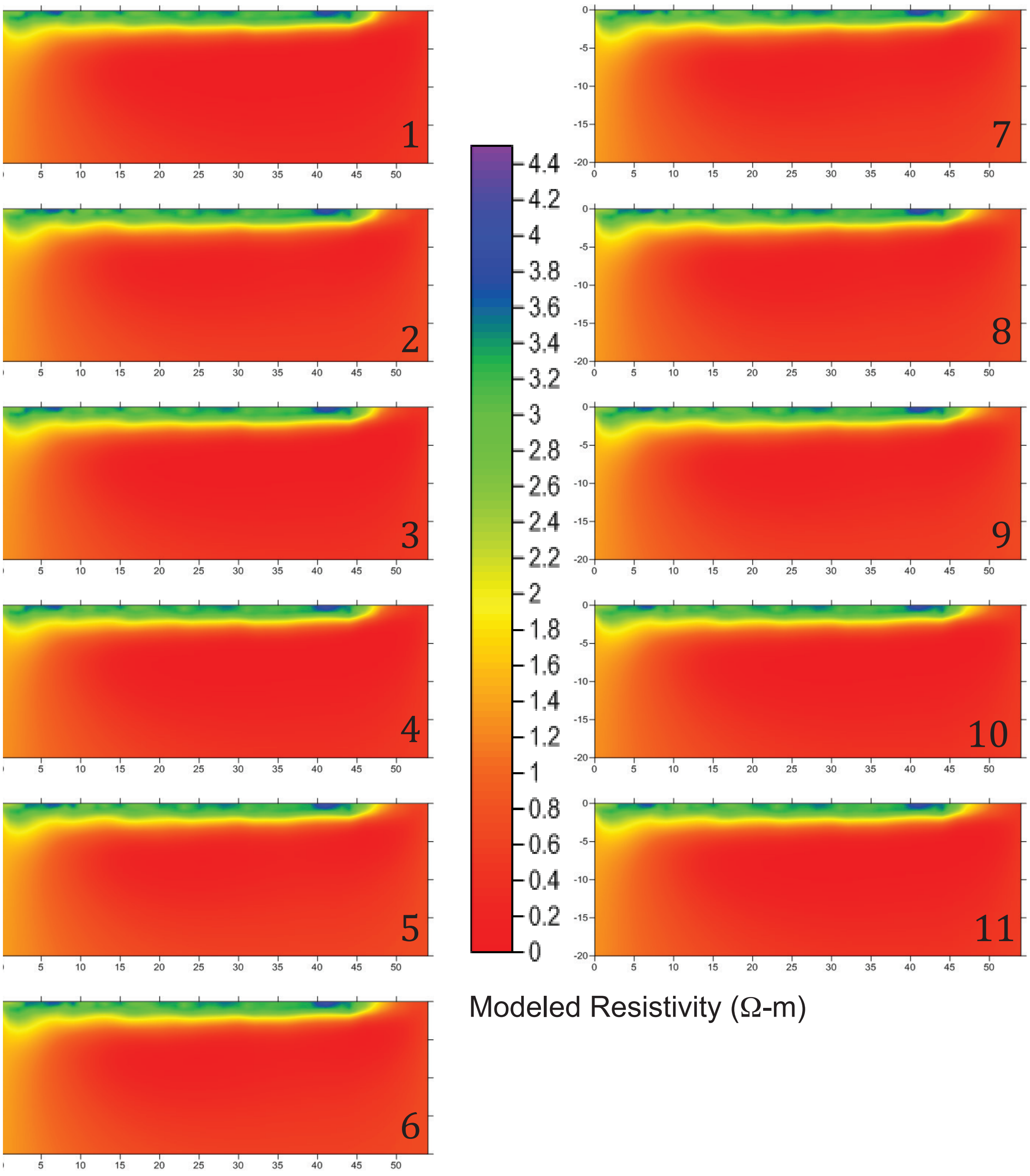

Figure 4. Modeled resistivity panels for each time step in the study produced using R2 and Surfer. Both the x and y axis are in units of meters. Values of resistivity are in Ω·m and are presented in logarithmic scale. Electrode 28 is located at 56 m, which is just below the high tide mark.

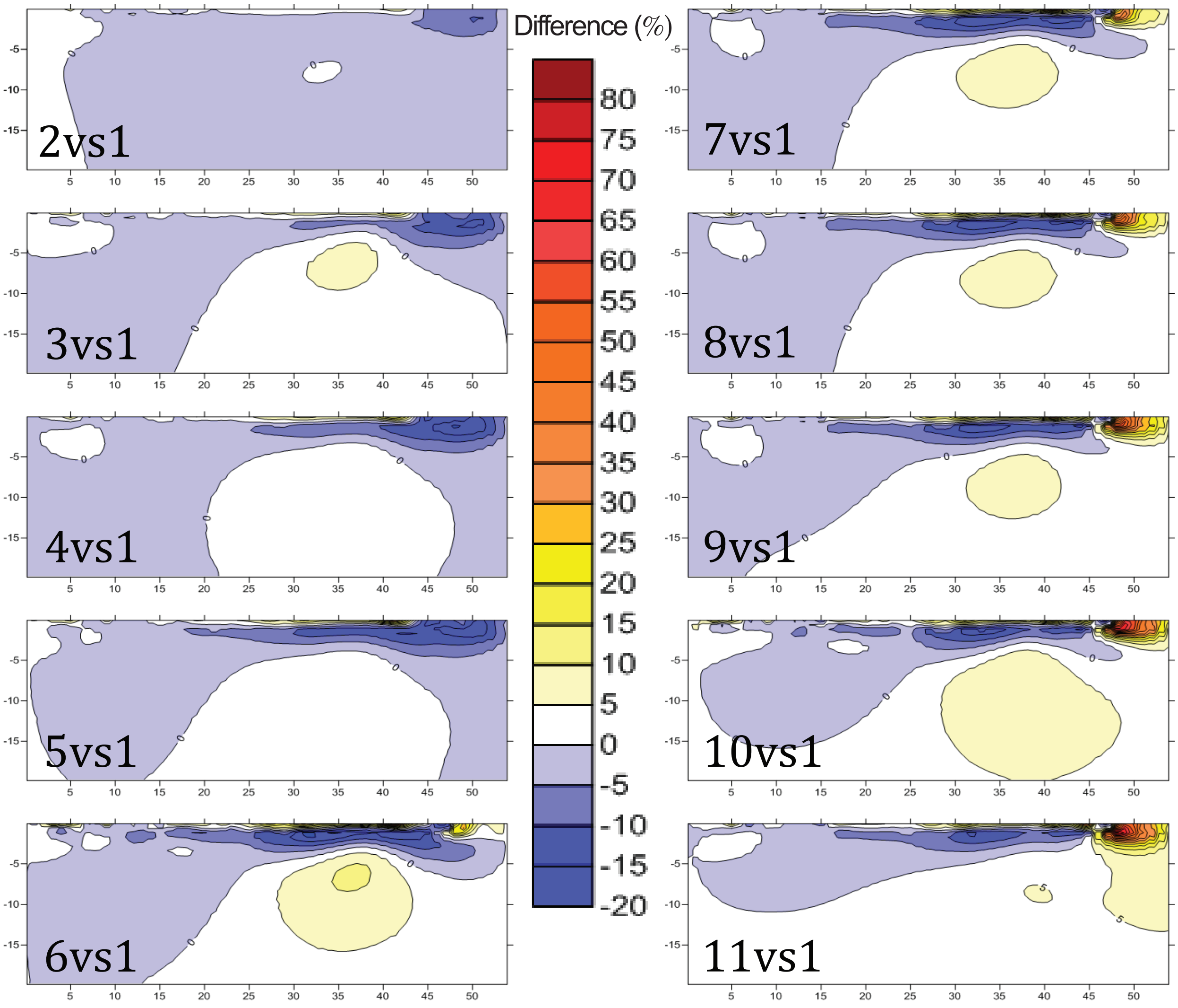

Figure 5. Modeled time-lapse resistivity panels for time step in the study compared to the initial conditions. Panels were produced using R2 and Surfer. Both the x and y axis are in units of meters. Values are presented as percent difference from the initial value. Electrode 28 is located at 56 m, which is just below the high tide mark.

phase with the tidal signal, and spatially variable in each time step. Generally speaking, they reveal a ‘pulse’ of lower resistivity fluid (i.e., marine water) moving landward followed by a dissipation of that marine water toward the end of the data collection. The distance of penetration of the salinity changes during this study appears to be approximately 40-45 m at this location and may be a limit imposed by the tidal range, the tide duration, and the rates of solute transport governed by the advection-dispersion equation in this aquifer matrix.

5. Conclusion

This preliminary study of time-lapse ERT methods along the coastline of San Salvador Island, Bahamas offers an interesting first glimpse into the nearshore behavior of a Holocene carbonate aquifer to tidal forcing. Results suggest that the water table oscillates in sync with the tides followed by a delayed advection/dispersion of marine waters. The attenuated tidal pulse penetrates approximately 40-45 m landward of the swash zone. The lag time between peak tide and minimum resistance is approximately three hours.

6. Acknowledgments

Work on this project was authorized by a permit granted from the Bahamas Environment, Science & Technology Commission. Sincere appreciation to Thomas Rothfus, Director of the Gerace Research Centre at the time of data collection, for his help with fieldwork logistics. Appreciation also for the constructive comments on an earlier draft of this manuscript by Dean Whitman of Florida International University.

7. References

Archie, G. E., 1952. Classification of carbonate reservoir rocks and petrophysical considerations. *American Association of Petroleum Geologists Bulletin* 36(2): 278–298.

Binley, A. and A. Kemna. 2005. Electrical Methods. *In* Y. Rubin and S. Hubbard [eds.], Hydrogeophysics, 129-156. Springer. Dordrecht, The Netherlands.

Culpepper, J. I. 2001. Determination of the presence of possible dissolution conduits using electrical resistivity, North Andros Island, Bahamas. Thesis, Wright State University, Dayton, Ohio.

Crump, M. A., and D. W. Gamble. 2006, Hydroclimatic analysis of a carbonate island pond through the development of a hydrologic landscape unit model. *Physical Geography* 27(6): 554-570.

Erdman, J. S., M. M. Key, Jr., and R. L. Davis. 1997. Hydrogeology of the Cockburn Town Aquifer, San Salvador Island, Bahamas, and the change in water quality resulting from the development of a resort community. *In* H. A. Curran, [ed.], Proceedings of the Eighth Symposium on the Geology of the Bahamas and Other Carbonate Regions, 47-58. Bahamian Field Station, San Salvador.

Gross, G. D. and A. W. G. Kunze. 1991. Electrical resistivity survey of freshwater lens in well field north of Cockburn Town, San Salvador, Bahamas. *In* R. J. Bain [ed], Proceedings of the Fifth Symposium on the Geology of the Bahamas, 91-101. Bahamian Field Station, Ft. Lauderdale, FL.

Kruse, S. E., M. R. Brudzinski, and T. L. Geib. 1998. Use of electrical and electromagnetic techniques to map seawater intrusion near the Cross-Florida Barge Canal. *Environmental and Engineering Geoscience* 4: 331-340.

Kunze, A. W. G., and W. G. Weir. 1987. Geoelectrical ground-water survey of the Sandy Hook area, San Salvador, Bahamas. *In* H. A. Curran [ed.], Proceedings of the 3rd Symposium on the Geology of the Bahamas, 81-89. Bahamian Field Station, San Salvador, The Bahamas.

Kunze, A. W. G., A. K. Sauter, and W. G. Weir. 1989. Geoelectrical survey of the Columbus Landings I region of San Salvador, Bahamas. *In* J. Mylroie [ed.], Proceedings of the 4th Symposium on the Geology of the Bahamas, 191-202. Bahamian Field Station, San Salvador, The Bahamas.

Kunze, A. W. G., T. J. Quick, and G. D. Gross. 1991. Measurements of tidal water table fluctuations in well field north of Cockburn Town, San Salvador, Bahamas. *In* R. J. Bain [ed.], Proceedings of the Fifth Symposium on the Geology of the Bahamas, 151-161. Bahamian Field Station, San Salvador, The Bahamas.

Kunze, A. W. G., and T. J. Quick. 1994. Tidal water level fluctuations in water wells on San Salvador Island, Bahamas. *Bulletin of the Association of Engineering Geologists* 31: 75-89.

Li, X., B. X. Hu, W. C. Burnett, I. R. Santos, J. P. Chanton. 2009. Submarine Ground Water Discharge Driven by Tidal Pumping in a Heterogeneous Aquifer. *Ground Water* 47(4): 558-568.

Meyerhoff, S. B., R. M. Maxwell, A. Revel, J. B. Martin, M. Karaoulis, and W.

D. Graham. 2014. Characterization of groundwater and surface water mixing in a semi-confined karst aquifer using time-lapse electrical resistivity tomography. *Water Resources Research* (50). doi: 10.1002/2013WR013991.

Michael, H. A., A. E. Mulligan, C. F. Harvey. 2005. Seasonal oscillations in water exchange between aquifers and the coastal ocean. *Nature* 436: 1145-1148.

Mylroie, J. E., J. L. Carew, and H. L. Vacher. 1995. Karst development in the Bahamas and Bermuda. *In* H. A. Curran and B. White [eds.]. Terrestrial and shallow marine geology of the Bahamas and Bermuda, 251–267. Geological Society of America Special Paper 300, Boulder, Colorado.

Roebuck, L., J. Pochatila, and T. Ortiz. 2004. Water Resource Assessment of the Bahamas. US Army Corps of Engineers, Mobile District & Topographic Engineering Center.

Russell S. A, L. J. Florea, and C. L. Stinson. 2010. Analysis of fresh water resources at the line hole well field, San Salvador Island, the Bahamas. *In* P. Kindler and D. Gamble [eds.], Proceedings of the 15th Symposium on the Geology of the Bahamas and other Carbonate Regions, 134-146. Gerace Research Centre, San Salvador, The Bahamas.

Sealey, N. 1994. Bahamian Landscapes: An introduction to the Geography of the Bahamas (Second Edition), Nassau, Bahamas: Media Publishing.

Townley, L. R. 1995. The response of aquifers to periodic forcing. *Advances in Water Resources* 18(3): 125-146.

Tucker, N. M. 2013. Analyzing Tidal Fluctuations in the Big Pine Key Freshwater Lens with Time-Lapse Resistivity. Thesis, Florida International University.

Urish, D. W., and R. K. Frohlich. 1990. Surface electrical resistivity in coastal groundwater exploration. *Geoexploration* 26(4): 267-289.

Vacher, H. L. 1988. Dupuit-Ghyben-Herzberg analysis of strip-island lenses. *Geological Society of America Bulletin* 100: 580-591.

Vacher, H. L. and T. Quinn. 2004. Geology and Hydrologeology of Carbonate Islands. Elsevier, Amsterdam, Netherlands.

Vacher, H. L., M. J. Wightman, and M. T. Stewart. 1992. Hydrology of meteoric diagenesis: effects of Pleistocene stratigraphy on freshwater lenses of Big Pine Key, Florida. *In* Coasts of the United States: Marine and Lacustrine Systems, 213-219. SEPM Special Publicaton 48. Tulsa, Oklahoma.

Whitaker, F. F., and P. L. Smart. 2004. Hydrogeology of the Bahamian Archipelago. *In* H. L. Vacher and T. Quinn [eds.], Geology and Hydrogeology of Carbonate Islands, 183-216. Elsevier, Amsterdam, The Netherlands.

Wolfe P. J., A. L. Adams, and C. K. Carney. 2001. A resistivity study of the freshwater lens profile across North Andros Island, Bahamas. *In* B. J. Greenstein and C. K. Carney [eds.], Proceedings of the 10th Symposium on the Geology of the Bahamas, 31-40. Gerace Research Centre, San Salvador, The Bahamas.

Yulia, A. 2011. Time-lapse electrical resistivity tomography applied to cave sustainability (Barbados) and groundwater exploration (Saint Lucia). Thesis, Massachusetts Institute of Technology. Boston, Massachusetts.